

## Regular article

# Enhanced protein crystallization around the metastable critical point\*

Pieter Rein ten Wolde, Daan Frenkel

FOM Institute for Atomic and Molecular Physics, Kruislaan 407, 1098 SJ Amsterdam, The Netherlands

Received: 4 June 1998 / Accepted: 3 September 1998 / Published online: 10 December 1998

**Abstract.** We report on a computer-simulation study of homogeneous crystal nucleation in a model for globular proteins. We find that the presence of a metastable vapour-liquid critical point drastically changes the pathway for the formation of a critical nucleus. But what is more important, the large density fluctuations near the critical point also lowers the free-energy barrier to nucleation and hence increases the nucleation rate. As the location of the vapour-liquid critical point can be controlled by changing the solvent conditions, our simulation results suggest a guided approach to protein crystallization.

**Key words:** Proteins – Crystallization – Nucleation – Computer simulation – Statistical physics

## 1 Introduction

Due to the rapid developments in biotechnology, more and more proteins are now being isolated. However, structural determination by X-ray crystallography is still a very time consuming process [1, 2]. One of the main reasons for this is that it is very hard to obtain good-quality protein crystals. In fact, obtaining the crystals is quite often more time consuming than determining the structure of the crystal, once it is obtained. It is for this reason that a lot of effort has been devoted to understanding the physical and chemical mechanisms that control the crystallization process. However, although crystallization conditions are usually systematically varied, the approach is not guided.

Three years ago, George and Wilson [3] reported on a very interesting observation. They found that the success of protein crystallization was correlated with the value of the second virial coefficient. The second virial coefficient

$B_2$  describes the lowest-order correction to van't Hoff's law for osmotic pressure,  $\Pi$ :

$$\frac{\Pi}{\rho k_B T} = 1 + B_2 \rho + (\text{terms of order } \rho^2), \quad (1)$$

where  $\rho$  is the number density of the dissolved molecules,  $k_B$  is Boltzmann's constant and  $T$  is the absolute temperature. Experimentally, the second virial coefficient of macromolecules is usually determined by static light scattering [4]. The value of  $B_2$  depends on the effective interaction between a pair of macromolecules [5]:

$$B_2 = \int 2\pi r^2 dr \left[ 1 - e^{-\frac{v(r)}{k_B T}} \right], \quad (2)$$

where  $v(r)$  is the interaction energy of a pair of molecules at distance  $r$ .

George and Wilson measured  $B_2$  for a number of proteins in various solvents. They found that for those solvent conditions that are known to promote crystallization,  $B_2$  was always restricted to a narrow "slot". If  $B_2$  was too large, crystallization did not occur at all, while for large and negative values of  $B_2$  protein aggregation, rather than crystallization, took place.

Two years ago, Rosenbaum et al. [6, 7] established a link between the observations of George and Wilson and the results of a computer-simulation study [8] in which the phase behaviour of colloid-polymer mixtures was studied. In these colloid-polymer mixtures, the range of the interaction between the colloids in solution can be controlled by tuning the radius-of-gyration of the polymer, i.e. by modifying the effective size of the polymer the range of the interaction between the colloids can be changed. Since the theoretical work of Gast et al. [9] and Lekkerkerker et al. [10] it has been known that the range of the attraction has a pronounced effect on the phase diagram. If the range of the interaction is long compared to the size of the colloids, then the phase behaviour of the colloids in solution resembles that of a simple atomic fluid, such as argon. Depending on the temperature and density, the colloids can occur in three phases: a dilute colloidal "gas" phase, a dense "liquid" phase and a crystalline phase (see Fig. 1A). However, if the range of the interaction is reduced, the liquid-vapour critical

\*Contribution to the Proceedings of Computational Chemistry and the Living World, April 20–24, 1998, Chambery, France

Correspondence to: P. R. ten Wolde

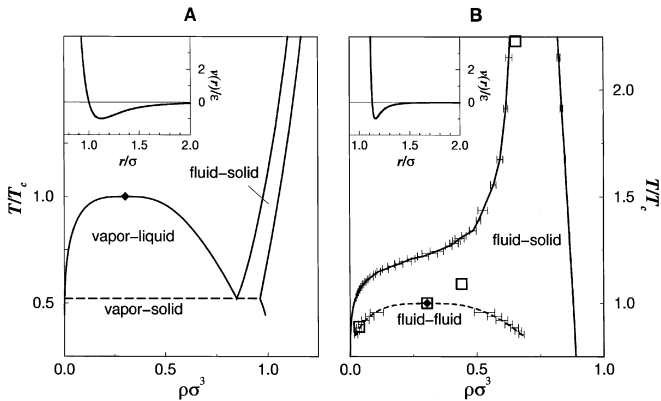


**Fig. 1** **A** Typical phase diagram of a molecular substance with a relatively long-ranged attractive interaction. The phase diagram shown here corresponds to the Lennard-Jones 6–12 potential  $v(r) = 4\epsilon[(\sigma/r)^{12} - (\sigma/r)^6]$  (solid curve in insert) [21]. The dashed line indicates the triple point. **B** Typical phase diagram of colloids with short-ranged attraction. The phase diagram was computed for the potential given in Eq. 4 (solid curve in insert), with  $\alpha = 50$ . In both figures, the temperature is expressed in units of the critical temperature  $T_c$ , while the number density is given in units  $\sigma^{-3}$ , where  $\sigma$ , the effective diameter of the particles, is defined in the expression for  $v(r)$ . The diamonds indicate the fluid-fluid critical points. In both figures, the solid lines indicate the equilibrium coexistence curves. The dashed curve in B indicates the metastable fluid-fluid coexistence. Crystal-nucleation barriers were computed for the points denoted by open squares

point shifts to lower temperatures. At some point, the liquid-vapour critical point will coalesce with the triple point (where vapour, liquid and solid coexist). If the range of attraction is then reduced even further, the liquid-vapour critical point will become metastable. Now only two stable phases remain, a fluid and a solid, and the liquid-vapour coexistence has become metastable (see Fig. 1B). We note here that this behaviour is not only found in theory, but also simulations [8] and in experiments [11, 12].

Why is this relevant to protein crystallization? First of all, the phase behaviour of a variety of globular proteins is of the kind shown in Fig. 1B [13–15]. In fact, Rosenbaum et al. showed that if the phase behaviour of these proteins is compared on an equal footing, then the phase diagrams can be mapped on top of each other [6, 7]. But what is more important, Rosenbaum and Zukoski [6, 7] clearly showed that the crystallization is strongly enhanced in a rather narrow region in the phase diagram. If the temperature is too high, crystallization is hardly observed at all, whereas if the temperature is too low, amorphous precipitation rather than crystallization occurs. Good crystals only form in a narrow window around the metastable critical point. The central question of this paper is: what is the origin of this protein crystallization window? Is it due to the presence of the metastable critical point? After all, at such a critical point, large density fluctuations can be expected and crystallization is essentially driven by density fluctuations. The aim of this paper is to show that the presence of the critical point is indeed essential for the formation of protein crystals. We

found that the critical point lowers the free-energy barrier to crystal nucleation and thereby increases the crystal-nucleation rate.

## 2 Method

The rate of crystal nucleation can be written as the product of two factors

$$J = k \exp[-\Delta G^*/k_B T] . \quad (3)$$

Here  $\Delta G^*$  is the free-energy barrier separating the stable solid phase from the metastable liquid, and  $k$  is a kinetic prefactor, which unless the system is close to a glass transition, only weakly depends on temperature. We have studied protein crystal nucleation away from the gelation curve. Hence, the variation in the nucleation rate is dominated by the variation in the height of the free-energy barrier. We have therefore computed the height of the free-energy barrier for different points in the phase diagram of a model globular protein.

In this model, the proteins interact via a suitable generalization of the Lennard-Jones potential:

$$v(r) = \frac{4\epsilon}{\alpha^2} \left( \frac{1}{[(r/\sigma)^2 - 1]^6} - \alpha \frac{1}{[(r/\sigma)^2 - 1]^3} \right) , \quad (4)$$

where  $\sigma$  denotes the hard-core diameter of the particles. This potential has a well depth  $\epsilon$ . The potential in Eq. (4) should be thought of as an effective interaction: it accounts for both direct and solvent-induced interactions between the globular proteins. The width of the attractive well can be adjusted by varying the parameter  $\alpha$ . We found that for  $\alpha \approx 50$ , the system reproduced the phase behaviour considered by Rosenbaum et al. [6]. Figure 1B shows the computed phase diagram. It is seen that the liquid-vapour coexistence curve is located in the metastable region some 20% below the equilibrium crystallization curve.

We computed the height of the free-energy barrier for the four points denoted by open squares in Fig. 1B. These points were chosen such that on the basis of classical nucleation theory the same height of the barrier could be expected. In classical nucleation theory the height of the barrier is given by

$$\Delta G^*/k_B T = \frac{16\pi\gamma^3}{3k_B T \rho^2 \Delta\mu^2} , \quad (5)$$

where  $\gamma$  is the surface free energy of the planar solid-liquid interface,  $\rho$  is the density of the crystal and  $\Delta\mu$  is the difference in chemical potential between a bulk solid and a bulk liquid. To estimate the difference in chemical potential we have made the common approximation

$$\Delta\mu \approx \Delta h(T_m - T)/T_m , \quad (6)$$

where  $\Delta h$  is the latent heat on melting and  $T_m$  is the melting temperature. To estimate  $\gamma$  we have used Turnbull's empirical rule that the surface free energy is proportional to the latent heat of melting [16].

The height of the free-energy barrier was computed with molecular dynamics, using the umbrella sampling scheme [17, 18]. In this scheme we compute the free energy of a nucleus as a function of its size. But what is a nucleus? As we are interested in crystallization, it seems natural to define the nucleus as a cluster of particles that are in a crystalline environment. As discussed in Ref. [17] each particle can be classified as either solid-like or liquid-like by analysing the local symmetry of its surroundings. If the distance between two particles is less than  $q_c = 1.5\sigma$ , the particles are considered to be connected; particles that are connected belong to the same cluster. However, as discussed above, we expect that crystallization near the critical point is influenced by large density fluctuations. We therefore identify a nucleus with a cluster of

connected particles that have a significantly higher local density than the particles in the remainder of the system. The size of this nucleus (be it solid-like or liquid-like) is denoted by  $N_\rho$ . The number of particles in this high-density cluster that are also in a crystalline environment is denoted by  $N_{\text{crys}}$ .

### 3 Discussion and conclusion

We have computed the free energy of a nucleus as a function of its size  $N_\rho$  and as a function of its crystallinity, denoted by  $N_{\text{crys}}$ . We will only discuss the free-energy landscape for the “lowest” two points (denoted by open squares) in Fig. 1B, as the results for the other two points are qualitatively similar to the lowest point for which we have computed the free-energy barrier. Figure 2 shows the free-energy landscapes. In a crystal nucleation event, the beginning is from the homogeneous liquid ( $N_\rho \approx N_{\text{crys}} \approx 0$ ), corresponding to a nucleus of “zero” size. The free energy is then increased until it reaches a saddle point, corresponding to the critical nucleus. From there on, the nucleus will grow spontaneously into a crystal.

We found that away from  $T_c$ , which is the temperature of the metastable liquid-vapour critical point, the path of the lowest free energy (indicated by the dashed curve) is one where the increase in  $N_\rho$  is proportional to the increase in  $N_{\text{crys}}$  (Fig. 2A). Such behaviour is expected if the initial nucleus is simply a small crystallite. However near  $T_c$ , critical density fluctuations lead to a striking change in the free-energy landscape (Fig. 2B). Now the lowest free-energy path initially runs parallel to the  $N_\rho$ -axis, i.e.  $N_\rho$  increases while  $N_{\text{crys}}$  is still essentially zero. This means that the first step towards the formation of a critical nucleus is not the formation of a small crystallite, but the formation of a high-density liquid-like droplet. Only when this droplet has reached a certain size does it start to crystallize in the core. From there on the increase in  $N_{\text{crys}}$  is proportional to  $N_\rho$ .

Clearly, the presence of large density fluctuations at the critical point has a drastic effect on the route to crystal nucleation. But, more importantly, it also lowers the free-energy barrier. The nucleation barrier at  $T_c$  is much lower than at either higher or lower temperatures, as shown in Fig. 3. As the nucleation rate depends exponentially on the height of the barrier (see Eq. 3), a reduction in the height of the barrier by some  $30k_B T$  corresponds to an increase in the nucleation rate by many orders of magnitude, i.e. by more than a factor of  $10^{13}$ . One interpretation of this observation is that near the critical point the wetting of the crystal nucleus by a liquid-like layer results in a value of the interfacial free energy  $\gamma$ , and therefore of the barrier height  $\Delta G^*$ , that is much lower than would be estimated on the basis of Turnbull’s rule. In fact, in a recent paper Haas and Drenth [19] note that the experimentally determined interfacial free energy of small protein crystals [20] is much smaller than the value predicted on the basis of their version of Turnbull’s rule.

Let us now consider the question of whether the reduction of the crystal nucleation barrier near  $T_c$  is of practical importance. At first sight, this is not obvious – after all, it is simple enough to lower the crystal nu-

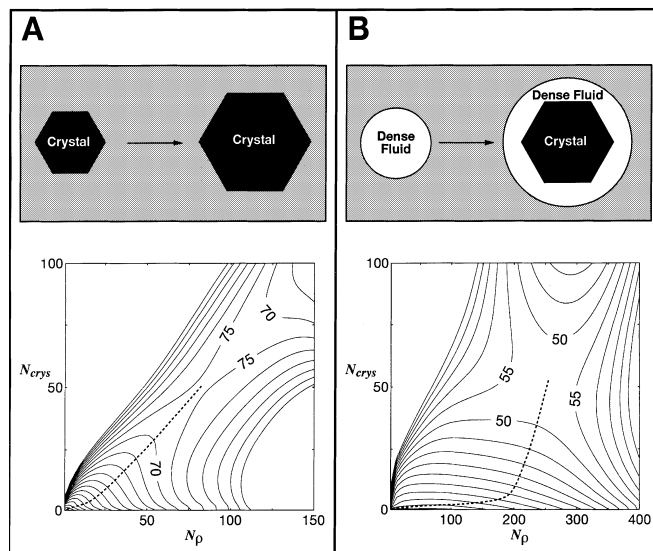


**Fig. 2A, B.** Contour plots of the free-energy landscape along the path from the metastable fluid to the critical crystal nucleus, for our system of spherical particles with short-ranged attraction. The curves of constant free energy are drawn as a function of  $N_\rho$  and  $N_{\text{crys}}$  (see text) and are separated by  $5k_B T$ . **A** The free-energy landscape well below the critical temperature ( $T/T_c = 0.89$ ). The lowest free-energy path to the critical nucleus is indicated by a dashed curve. This curve corresponds to the formation and growth of a highly crystalline cluster. **B** As (A), but for  $T = T_c$ . In this case, the free-energy valley (dashed curve) first runs parallel to the  $N_\rho$  axis (formation of a liquid-like droplet), and then moves towards a structure with a higher crystallinity (crystallite embedded in a liquid-like droplet). The free-energy barrier for this route is much lower than the one in (A)

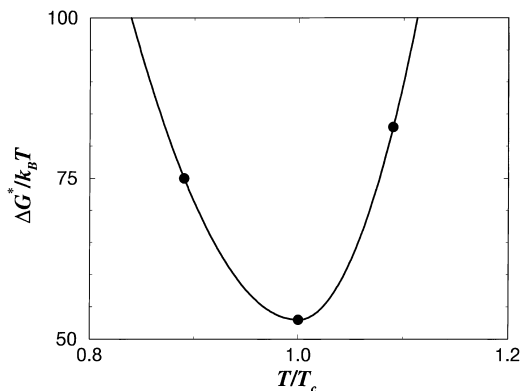


**Fig. 3.** Variation of the free-energy barrier for homogeneous crystal nucleation, as a function of  $T/T_c$ , in the vicinity of the critical temperature. The solid curve is a guide to the eye. The nucleation barrier at  $T = 2.23T_c$  is  $128k_B T$  and is not shown in this figure. If Turnbull’s phenomenological rule for  $\gamma$  is right [16], Eq. 5 would predict a constant nucleation barrier. But the simulations show that the nucleation barrier goes through a minimum around the metastable critical point (see text)

cleation barrier by quenching the solution deeper into the metastable region below the solid-liquid coexistence curve. However, simply quenching the solution, i.e. increasing the supersaturation, has two side effects: deep quenches often result in the formation of amorphous

aggregates [3, 12]. Secondly, in a deep quench the thermodynamic driving force for crystallization ( $\mu_{\text{liq}} - \mu_{\text{cryst}}$ ) is also enhanced. As a consequence, crystallites that do nucleate will grow rapidly and far from perfectly. Often, the resulting imperfections lead to a “self-poisoning” of the crystal growth [2]. Hence, the nice feature of crystallization near the metastable critical point is that it is possible to obtain critical nuclei and hence crystals at relatively moderate supersaturations. At this metastable critical point the conditions for protein crystallization are optimal. For lower densities the supersaturation is lower and hence the nucleation rate is lower, whereas for higher densities, as indicated above, glass formation can hinder the crystallization process.

Finally, we would like to point out that the mechanism described here is probably quite general. Of course, the details of the interaction potential will affect the phase diagram. However, we believe that the general features of the phase diagram shown in Fig. 1B are likely to be the rule rather than the exception for compact macromolecules. We suggest that as long as a metastable critical point is located “underneath” the equilibrium coexistence curve, critical density fluctuations will facilitate the formation of ordered structures. Furthermore, the location of the critical point can be controlled by adjusting the solvent conditions (e.g. by the addition of non-ionic polymer). It should be tuned such that the fluid-fluid critical point is located just below the sublimation curve. If experiments are performed near this metastable critical point, one will selectively speed up the rate of crystal nucleation, but not the rate of crystal growth, nor the rate at which amorphous aggregates form.

*Acknowledgements.* This work was supported by Scheikundig Onderzoek Nederland (SON) and by Fundamenteel Onderzoek der Materie (FOM) with financial aid from Nederlandse Organisatie voor Wetenschappelijk Onderzoek (NWO) and computer time provided by Nationale Computer Faciliteiten (NCF).

## References

1. McPherson A (1982) Preparation and analysis of protein crystals. Krieger Malabar
2. (a) Durbin SD, Feher G (1996) *Ann Rev Phys Chem* 47: 171; (b) Rosenberger F (1996) *J Cryst Grow* 166: 40
3. George A, Wilson WW (1994) *Acta Crystallogr D* 50: 361
4. Richards EG (1980) An introduction to physical properties of large molecules in solution. Cambridge University Press, Cambridge, UK
5. See for example Hill TL (1986) An introduction to Statistical Thermodynamics, Dover Publications, New York
6. Rosenbaum D, Zamora PC, Zukoski CF (1996) *Phys Rev Lett* 76: 150
7. Rosenbaum DF, Zukoski CF (1996) *J Cryst Grow* 169: 752
8. Hagen MHJ, Frenkel D (1994) *J Chem Phys* 101: 4093
9. (a) Gast AP, Russell WB, Hall CK (1983) *J Colloid Interface Sci* 96: 251; (b) Gast AP, Russell WB, Hall CK (1983) *J Colloid Interface Sci* 109: 161
10. Lekkerkerker HNW, Poon WCK, Pusey PN, Stroobants A, Warren PB (1992) *Europhys Lett* 20: 559
11. Ilett SM, Orrock A, Poon WCK, Pusey PN (1995) *Phys Rev E* 51: 1344
12. (a) Poon WCK, Pirie AD, Pusey PN (1995) *Faraday Discuss* 101: 65; (b) Poon WCK (1997) *Phys Rev E* 55: 3762
13. (a) Berland CR, Thurston GM, Kondo M, Broide ML, Pande J, Ogun OO, Benedek GB (1992) *Proc Natl Acad Sci USA* 89: 1214; (b) Asherie N, Lomakin A, Benedek GB (1996) *Phys Rev Lett* 77: 4832
14. Broide ML, Tominc TM, Saxowsky MD (1996) *Phys Rev E* 53: 6325
15. Muschol M, Rosenberger F (1997) *J Chem Phys* 107: 1953
16. Kelton KF (1991) In: Ehrenreich H, Turnbull D (eds) *Crystal nucleation in liquids and glasses* vol 45, Academic Press, Boston, p. 75. As shown in this reference, the constant of proportionality is system specific
17. (a) Ten Wolde PR, Ruiz-Montero MJ, Frenkel D (1995) *Phys Rev Lett* 75: 2714; (b) Ten Wolde PR, Ruiz-Montero MJ, Frenkel D (1996) *J Chem Phys* 104: 9932
18. Torrie GM, Valleau JP (1974) *Chem Phys Lett* 28: 578
19. Haas C, Drenth J (1995) *J Cryst Grow* 154: 126
20. (a) Malkin AJ, McPherson A (1992) *J Cryst Grow* 128: 1232; (b) Malkin AJ, McPherson A (1993) *J Cryst Grow* 133: 29
21. Hansen JP, Verlet HL (1969) *Phys Rev* 184: 151